REPORT DOCUMENTATION PAGE

Form Approved OMB NO. 0704-0188

1. REPORT DATE (DD-MM-YYYY)	2. REPORT TYPE	3. DATES COVERED (From - To)
01-08-2012	Final Report	1-Sep-2011 - 31-May-2012

4. TITLE AND SUBTITLE
1.55 μm In(Ga)N Nanowire Lasers on Silicon

5a. CONTRACT NUMBER
W911NF-11-1-0450

5b. GRANT NUMBER

5c. PROGRAM ELEMENT NUMBER
611102

6. AUTHORS
Zetian Mi

5d. PROJECT NUMBER

5e. TASK NUMBER

5f. WORK UNIT NUMBER

7. PERFORMING ORGANIZATION NAMES AND ADDRESSES
McGill University
Office of Sponsored Research
McGill University
-

8. PERFORMING ORGANIZATION REPORT NUMBER

9. SPONSORING/MONITORING AGENCY NAME(S) AND ADDRESS(ES)
U.S. Army Research Office
P.O. Box 12211
Research Triangle Park, NC 27709-2211

10. SPONSOR/MONITOR'S ACRONYM(S)
ARO

11. SPONSOR/MONITOR'S REPORT NUMBER(S)
60781-EL-II.4

12. DISTRIBUTION AVAILIBILITY STATEMENT
Approved for Public Release; Distribution Unlimited

13. SUPPLEMENTARY NOTES
The views, opinions and/or findings contained in this report are those of the author(s) and should not contrued as an official Department of the Army position, policy or decision, unless so designated by other documentation.

14. ABSTRACT
The development of Si photonics and the implementation of inter- and intra-chip optical interconnects has been severely hampered by the lack of a suitable light source on Si. In this project, we propose to develop In(Ga)N nanowire lasers on a Si-platform, with emission in the spectral range of 1.55 um, for chip-level optical communication applications. Nearly dislocation-free In(Ga)N nanowire heterostructures are formed directly on Si substrates with the use of an in situ deposited In seeding layer as a catalyst. We have recently achieved, for the first

15. SUBJECT TERMS
nanowire, laser, Si photonics

16. SECURITY CLASSIFICATION OF:			17. LIMITATION OF ABSTRACT	15. NUMBER OF PAGES	19a. NAME OF RESPONSIBLE PERSON
a. REPORT	b. ABSTRACT	c. THIS PAGE			Zetian Mi
UU	UU	UU	UU		19b. TELEPHONE NUMBER: 514-398-7114

Standard Form 298 (Rev 8/98)
Prescribed by ANSI Std. Z39.18

Report Title

1.55 μm In(Ga)N Nanowire Lasers on Silicon

ABSTRACT

The development of Si photonics and the implementation of inter- and intra-chip optical interconnects has been severely hampered by the lack of a suitable light source on Si. In this project, we propose to develop In(Ga)N nanowire lasers on a Si-platform, with emission in the spectral range of 1.55 um, for chip-level optical communication applications. Nearly dislocation-free In(Ga)N nanowire heterostructures are formed directly on Si substrates with the use of an in situ deposited In seeding layer as a catalyst. We have recently achieved, for the first time, nearly intrinsic and Si-doped InN nanowires as well as nanowire LEDs with the highest internal quantum efficiency ever reported. In this project, we will first investigate the design and selective area growth of InGaN core-shell nanowire laser heterostructures. Both optically pumped and electrically single InGaN nanowire lasers on Si will be fabricated and characterized, with the objective to achieve an ultralow threshold (< 100 uA) and relatively high output power (>100 μW).

Enter List of papers submitted or published that acknowledge ARO support from the start of the project to the date of this printing. List the papers, including journal references, in the following categories:

(a) Papers published in peer-reviewed journals (N/A for none)

Received	Paper
2012/08/01 10 2	Shouvik Mukherjee, Pablo Bianucci, M. Hadi Tavakoli Dastjerdi, Philip J. Poole, Zetian Mi. Self-organized InAs/InGaAsP quantum dot tube lasers, Applied Physics Letters, (2012): 0. doi: 10.1063/1.4737425
2012/08/01 10 1	S. Zhao, S. Fathololoumi, K. H. Bevan, D. P. Liu, M. G. Kibria, Q. Li, G. T. Wang, Hong Guo, Z. Mi. Tuning the Surface Charge Properties of Epitaxial InN Nanowires, Nano Letters, (06 2012): 0. doi: 10.1021/nl300476d
2012/08/01 10 3	Kai Cui, Saeed Fathololoumi, Md Golam Kibria, Gianluigi A Botton, Zetian Mi. Molecular beam epitaxial growth and characterization of catalyst-free InN/In, Nanotechnology, (03 2012): 85205. doi: 10.1088/0957-4484/23/8/085205

TOTAL: 3

Number of Papers published in peer-reviewed journals:

(b) Papers published in non-peer-reviewed journals (N/A for none)

Received	Paper

TOTAL:

Number of Papers published in non peer-reviewed journals:

(c) Presentations

1. P. Bianucci, M. H. Tavakoli?Dastjerdi, S. Mukherjee, M. Djavid, P. J. Poole, Z. Mi “An optically pumped InGaAsP/InP quantum dot rolled?up microtube laser”, American Physical Society March Meeting, Boston, MA, Feb. 27 - March 2, 2012.

2. Invited: Z. Mi, P. Bianucci, M. H. T. Dastjerdi, S. Mukherjee, M. Djavid, and P. Poole, “Rolled-up 1.55 μm Semiconductor Quantum Dot Tube Lasers”, 221st Electrochemical Society Meeting, Seattle, WA, USA, May 6-11, 2012.

3. S. Zhao, S. Fathololoumi, K. H. Bevan, D. Liu, Md. G. Kibria, Q. Li, G. Wang, H. Guo, and Z. Mi, “Tuning the surface charge properties of InN nanowires,” Electronic Materials Conference, Pennsylvania State University, June 20-22, 2012.

4. S. Zhao, S. Fathololoumi, K. Cui, Q. Li, G. Wang, and Z. Mi, “Molecular beam epitaxial growth and characterization of nearly intrinsic and Si-doped InN nanowires,” Photonics West Conference, San Francisco, CA, Jan. 21-26, 2012.

Number of Presentations: 4.00

Non Peer-Reviewed Conference Proceeding publications (other than abstracts):

Received Paper

TOTAL:

Number of Non Peer-Reviewed Conference Proceeding publications (other than abstracts):

Peer-Reviewed Conference Proceeding publications (other than abstracts):

Received Paper

TOTAL:

Number of Peer-Reviewed Conference Proceeding publications (other than abstracts):

(d) Manuscripts

Received Paper

TOTAL:

Number of Manuscripts:

Books

Received Paper

TOTAL:

Patents Submitted

Patents Awarded

Awards

Zetian Mi received the Christophe Pierre Award for Research Excellence in the Faculty of Engineering at McGill University in 2012.

Graduate Students

NAME	PERCENT_SUPPORTED	Discipline
Songrui Zhao	0.50	
FTE Equivalent:	**0.50**	
Total Number:	**1**	

Names of Post Doctorates

NAME	PERCENT_SUPPORTED

FTE Equivalent:
Total Number:

Names of Faculty Supported

NAME	PERCENT_SUPPORTED

FTE Equivalent:
Total Number:

Names of Under Graduate students supported

NAME	PERCENT_SUPPORTED

FTE Equivalent:
Total Number:

Student Metrics

This section only applies to graduating undergraduates supported by this agreement in this reporting period

The number of undergraduates funded by this agreement who graduated during this period:	0.00
The number of undergraduates funded by this agreement who graduated during this period with a degree in science, mathematics, engineering, or technology fields:.....	0.00
The number of undergraduates funded by your agreement who graduated during this period and will continue to pursue a graduate or Ph.D. degree in science, mathematics, engineering, or technology fields:.....	1.00
Number of graduating undergraduates who achieved a 3.5 GPA to 4.0 (4.0 max scale):	0.00
Number of graduating undergraduates funded by a DoD funded Center of Excellence grant for Education, Research and Engineering:	0.00
The number of undergraduates funded by your agreement who graduated during this period and intend to work for the Department of Defense	0.00
The number of undergraduates funded by your agreement who graduated during this period and will receive scholarships or fellowships for further studies in science, mathematics, engineering or technology fields:	0.00

Names of Personnel receiving masters degrees

NAME

Total Number:

Names of personnel receiving PHDs

NAME

Total Number:

Names of other research staff

NAME	PERCENT_SUPPORTED

FTE Equivalent:
Total Number:

Sub Contractors (DD882)

Inventions (DD882)

Scientific Progress

See Attachment

Technology Transfer

Final Project Report

1. Statement of the Problem Studied

Electrically injected nanoscale coherent light sources on Si, with operation wavelengths at 1.3 – 1.55 μm and controlled emission properties, are required for future applications in chip-level optical interconnects. Recently, InN-based nanowire heterostructures have emerged as a highly promising candidate for high performance nanophotonic devices on Si. In(Ga)N exhibit extraordinary attributes, including tunable energy bandgap from 0.7 eV to 3.4 eV, extremely large absorption coefficient ($\geq 2\times10^5$ cm^{-1}) and large material gain in the C- and L-bands, and very high electron saturation velocity (2×10^8 cm/s), that are ideally suited for applications in chip-level ultrahigh-speed lasers and photodetectors. To date, however, InN-based devices in the near-infrared spectral range have remained largely unexplored, which is in direct contrast to the relatively mature GaN-based devices, such as light emitting diodes (LEDs) and lasers that have transformed the solid state lighting technology. This has been primarily limited by the difficulty in achieving high quality InN, due to the lack of suitable substrates. In addition, InN has the lowest conduction band minimum of any reported semiconductor and, as a consequence, defects and impurities are generally donor-like. For this reason, the currently reported InN is typically n-type degenerate even for nominally undoped structures. The grown surfaces of InN are also characterized by problematic, uncontrollable surface electron accumulation, the origins of which have remained a subject of intense debate. The lack of intrinsic InN, the uncontrolled surface charge properties, and the difficulty in realizing p-type conductivity has been recognized as the major obstacles for the practical device applications of III-nitride semiconductors in the near-infrared spectral range. By virtue of the effective lateral stress relaxation, nearly defect-free nanowire heterostructures can be monolithically grown on Si-platform, rendering them as highly promising building blocks for high performance nanophotonic devices on Si. Additionally, the use of nanowires provides an effective approach to scale down the dimensions of future devices and systems. It can also significantly enhance the operation bandwidth of nanophotonic devices, due to the greatly reduced parasitic capacitance and carrier transient time.

In this report, we summarize our work on the design, molecular beam epitaxial growth, and characterization of InGaN nanowire heterostructures on Si for applications in nanoscale lasers. We describe our achievement of intrinsic InN nanowires, the precise control over the surface charge properties, and the demonstration of InN/InGaN core/shell nanowires. In addition, we also report on the demonstration of 1.55 μm self-organized InAs/InGaAsP quantum dot tube lasers.

2. Summary of the Most Important Results

2.1. Molecular Beam Epitaxial Growth and Characterization of Intrinsic InN Nanowires

In this experiment, InN nanowires were grown on Si (111) substrates by a Veeco Gen-II radio-frequency plasma-assisted molecular beam epitaxial growth system under nitrogen-rich conditions. A thin (~ 0.6 nm) In layer was deposited on the substrate surface before introducing nitrogen, compared to the conventional spontaneous formation of InN nanowires. The In layer forms nanoscale droplets at elevated temperatures, which can promote the subsequent formation and nucleation of InN nanowires. The growth conditions for InN nanowires included: a substrate

temperature of ~ 480 °C, an In flux of ~ 6×10^{-8} torr, a nitrogen flow rate of ~ 1.0 sccm, and a RF plasma forward power of ~ 350 W. Under optimum growth conditions, InN nanowires can exhibit a non-tapered wurtzite structure (*i.e.* identical top and bottom sizes for both undoped and Si-doped InN nanowires). Shown in Figure 1(a) is the scanning electron microscopy (SEM) image of InN nanowire arrays on Si(111) taken with a 45-degree angle, which exhibit a well-defined hexagonal morphology. This near-perfect morphology and phase purity can also be achieved for wires with relatively large dimensions (see Figure 1(b)). InN nanowires in this study have lengths in the range of ~ 0.7 μm to ~ 4 μm, depending on the growth duration. The nanowires are oriented along the [0001] polar direction, with their sidewalls being non-polar *m*-planes. Such non-tapered nanowires are nearly free of structural defects (i.e. dislocations and stacking faults), thereby minimizing unintentional *n*-type doping due to defects.

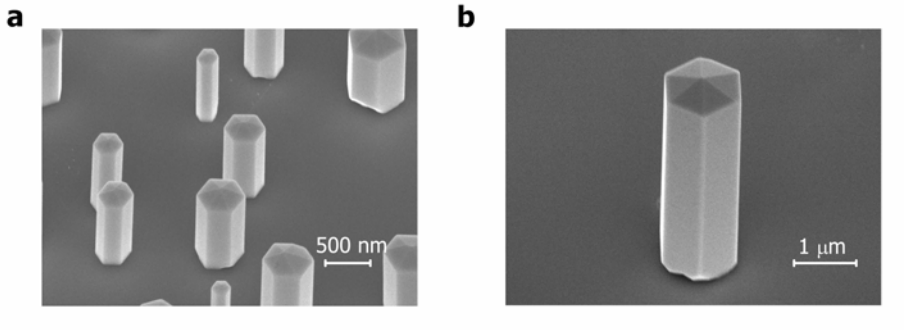

Figure 1: Scanning electron microscopy images of non-tapered undoped InN nanowires grown on Si (111) substrate. (a) Short duration growth nanowires (lengths ~ 0.7 μm). (b) Relatively long growth duration nanowires (lengths ~ 4 μm).

Micro-PL measurements were performed at both low temperature and room temperature. The non-tapered undoped InN nanowires, in this work, can exhibit an extremely narrow PL spectral linewidth of ~ 9 meV under an excitation power of ~ 0.5 μW at 10 K, shown in Figure 2(a). This linewidth is nearly a factor of 5 to 10 times smaller, compared to the commonly reported values for the conventional *n*-type degenerate InN nanowires or films, suggesting the superior quality of such non-tapered InN nanowires. The peak energy position at ~ 0.675 eV also agrees reasonably well with the band gap of InN in this temperature range.

Recent studies have suggested that the residual doping of InN can be approximately derived by analyzing the PL spectral linewidth at low temperatures. The same approach was employed here. To first order, for such InN nanowires with a PL spectral linewidth of $\Gamma \sim 9$ meV, the total electron density, *n*, at 10 K was estimated to be ~ 2.5×10^{16} cm^{-3} (when the inhomogeneous broadening is neglected). However, by considering the inhomogeneous broadening, Γ_{ih}, a lower value of *n* can be derived from $n_0(1-\Gamma_{ih}/\Gamma)^{1/\alpha}$, where $\alpha \approx 0.5$ and n_0 is the residual dopant concentration. Assuming an inhomogeneous broadening of ~ 5 meV (which represents a lower limit on the values normally measured for III-V compound semiconducting nanowires grown on Si) for the presented InN nanowires, we obtain $n \sim 4\times10^{15}$ cm^{-3}. Since the estimated value may include residual doping, n_0, and photogenerated electrons, n-n_0, we therefore conclude that such non-tapered undoped InN nanowires exhibit an extremely low (less than 4×10^{15} cm^{-3}) residual electron density. This value is nearly two to three orders of magnitude smaller than the commonly reported values for InN nanowires and films.

The high quality of such undoped InN nanowires is further evidenced by the presence of exciton-medicated PL emission. As shown in Figure 2(b), the PL peak energy position is nearly independent of the optical excitation power for well over 4 decades of intensity variation, and the emission spectra are highly symmetric. This is fundamentally distinct from the Mahan excitons in *n*-type degenerate InN, which generally leads to a PL peak energy significantly larger than the band gap of InN. Detailed power dependent integrated PL intensity study suggests the PL emission is mediated by excitons at low temperatures, i.e., if the PL spectra are mediated by exciton-line emission, then one would expect a linear power dependence in the integrated PL intensity. This is indeed the case as shown in Figure 2(c), where the integrated PL intensity exhibits a linear dependence with respect to the excitation power over 3 orders of magnitude (The deviation from linearity under very high excitation conditions can be attributed to optical heating). Collectively, these results suggest that the PL spectra are mediated by exciton-line emission.

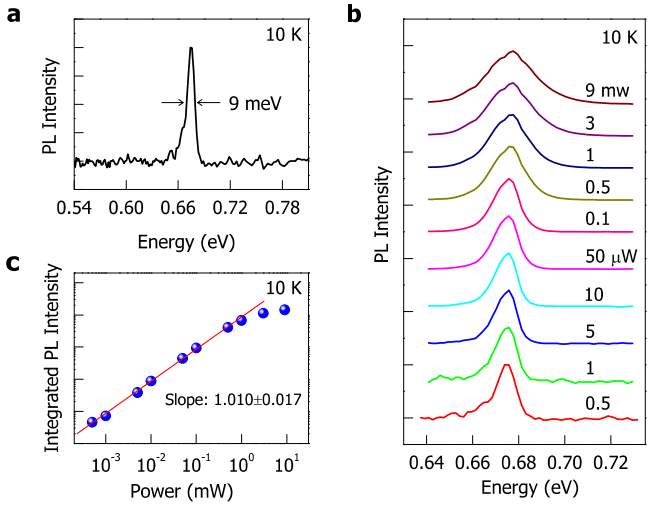

Figure 2: Micro-PL spectra of intrinsic InN nanowires. (a) Spectrum measured at 10 K under an excitation power of ~ 0.5 μW. (b) Power dependent PL spectra of the same intrinsic InN nanowires measured at 10 K. (c) Excitation power dependent integrated PL intensity at 10 K derived from (b) (displayed in logarithm scale). Each spectrum in (a) and (b) was normalized by its individual peak intensity and shifted vertically for display purposes.

2.2. Tuning the Surface Charge Properties of InN Nanowires

To date, precise control over nanowire doping, as well as the surface charge properties, has remained a near universal materials challenge. InN has the lowest conduction band minimum (CBM) of any reported semiconductor, the CNL is positioned at ~ 1.2 eV above the CBM. Hence, defects and impurities in these compounds are generally donor-like, leading to extremely high electron densities even in nominally undoped structures. Common to these materials is the near-universal observation of a two-dimensional electron gas (2DEG) at the grown surfaces of both thin film and nanowire structures, the origins of which have remained a subject of intense debate. For these reasons, the achievement of intrinsic and *p*-type InN, as well as precise control over their surface charge properties, has remained an elusive goal.

The achievement of intrinsic InN nanowires enables us to unveil, for the first time, the fundamental surface charge properties of InN nanowires, which are investigated directly by the angle-resolved X-ray photoelectron spectroscopy (XPS). Illustrated in Figure 3(a) is the measurement of the near-surface Fermi-level (E_F) relative to the position of the valence band maximum (VBM). It can be seen that E_F lies at ~ 0.5 eV above the VBM, suggesting the minimal downward band bending and the absence of electron accumulation on the sidewalls of InN nanowires. The highly symmetric In-3$d_{5/2}$ and N-1*s* XPS spectra, shown in the inset of Figure 3(a), further suggest the negligible levels of impurity bondings (such as In-O, N-H or N-C) associated with the surface electron accumulation. This is the first demonstration that the surface two-dimensional electron gas (2DEG) formation and E_F pinning is absent at the non-polar *grown* surfaces of any InN structure since this prediction was made by Van de Walle *et al*. in 2007, which is in direct contrast to the problematic 2DEG formation universally observed at the grown surfaces of *n*-type degenerate InN. With this demonstration we have discovered that the commonly measured large surface electron accumulation and Fermi-level pinning at the non-polar grown surfaces is *not* a fundamental property of InN.

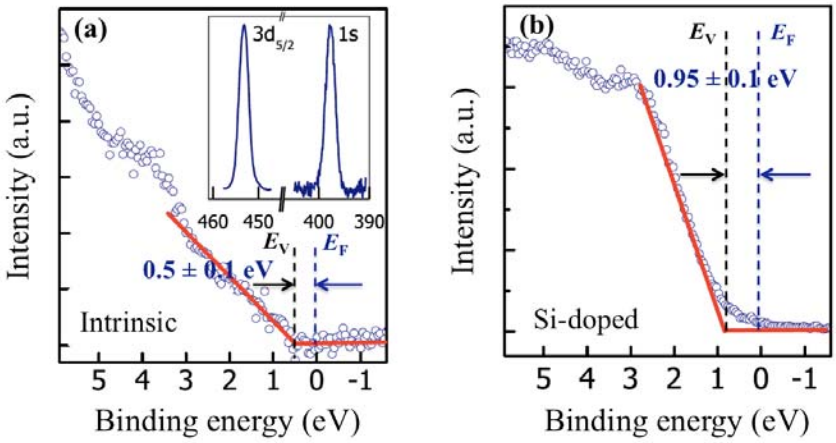

Figure 3: Angle-resolved XPS spectra[16] of (a) intrinsic and (b) Si-doped InN nanowires. The spectra are measured from the lateral surfaces (*m*-plane) of [0001]-oriented InN nanowires. The inset of (a) shows the spectra of In-3$d_{5/2}$ and N-1*s* orbitals measured from the lateral surfaces, suggesting the absence of In-O related bonds.

Significantly, we have also demonstrated that the surface charge properties of InN nanowires can be tuned by controlled n-type doping. This is evidenced by the XPS experiments on the Si-doped InN nanowires with an average doping concentration of ~ 5×10^{17} cm^{-3}. As can be seen from Figure 3(b), E_F lies ~ 0.95 eV above the VBM. Given a bandgap of ~ 0.65 eV at room temperature, the E_F of Si-doped InN nanowires is located at ~ 0.3 eV above the CBM. This indicates the presence of a high-density 2DEG (> 6×10^{12} cm^{-2}), which is significantly larger than the bulk doping concentration. This observation is similar to the commonly reported 2DEG that forms at the surfaces of unintentionally *n*-type doped InN nanowires and thin films; here, however, it was obtained by the controlled Si-doping. The tuning of surface charge properties is well captured by the effective mass and *ab-initio* calculations, which is closely related to the dopant surface segregation.

2.3. InN:Mg Nanowires

Due to the presence of surface electron accumulation, the realization of p-type conductivity in InN has remained an elusive goal. With the achievement of intrinsic InN nanowires, both within the bulk and at the grown surfaces, it is possible to obtain p-doped InN nanowires. InN:Mg nanowires are grown on Si(111) substrate using the afore-described catalyst-free method. The photoluminescence properties of such nanowires are investigated. Illustrated in Figure 4, under relatively low excitation conditions, the photoluminescence emission measured at ~ 6 K is dominated by a low energy peak at ~ 0.6 eV, which is ascribed to Mg-dopant associated acceptor energy level(s) transition. With increasing pumping power, the band-to-band transition becomes appreciably more important, due to the saturation of acceptor energy level(s). The energy separation between the two peaks is ~ 60 meV, which is consistent with the Mg acceptor activation energy in InN epi-layers in previous reports. Various electrical methods are currently being explored to confirm p-type conductivity in InN nanowires.

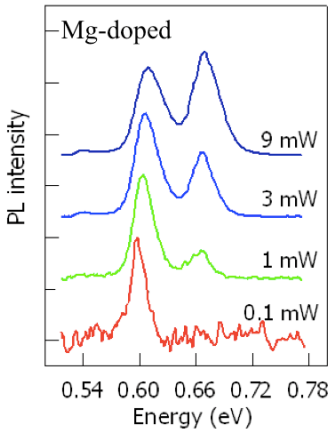

Figure 4: Power dependent PL spectra of Mg-doped InN nanowires measured at 6 K.

2.4. InN/InGaN Core-Shell Nanowire Heterostructures

To achieve high efficiency InN-based nanowire LEDs and lasers, it is essential to develop InN/InGaN core-shell nanowire heterostructures that can provide effective carrier confinement and bandgap engineering. The recently demonstrated InN/InGaN core-shell nanowire structures are illustrated in Figure 5(a), wherein the InN nanowires are covered by an InGaN shell on the side-wall and top regions. Such core/shell nanowire structures are achieved by depositing InGaN on InN nanowire template at a slightly higher substrate temperature of ~ 500 °C, which can enhance the surface diffusion of Ga adatoms. The elemental map for In derived from the energy dispersive X-ray spectrometry (EDXS) analysis of an individual InN/InGaN nanowire heterostructure is shown in Figure 5(b). The color-coded map (inset) with the In in green and the Ga in red confirms that the Ga distribution is on the periphery of the nanowire, which provides a direct evidence for the core-shell configuration. The InGaN shell is expected to provide superior carrier confinement for the InN core. A record internal quantum efficiency of ~ 62% is measured from such nanowire heterostructures at room temperature, shown in Figure 6. The use of such unique radial core/shell nanowire heterostructures for laser applications is being investigated.

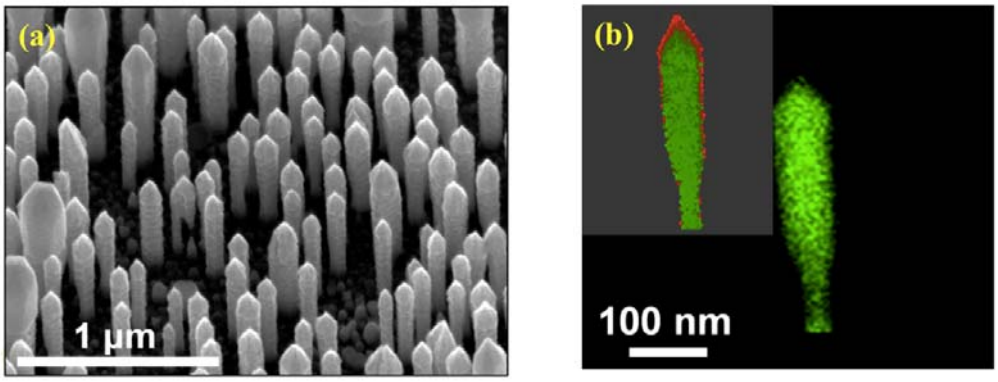

Figure 5: (a) SEM image taken with a 45-degree angle, showing the morphology and orientation of the InN/InGaN nanowires grown on Si (111) substrate. (b) In map derived from the EDXS analysis of an individual InN/InGaN nanowire heterostructure. The color-coded map (inset) with the In in green and the Ga in red shows that the Ga distribution is on the periphery of the nanowire.

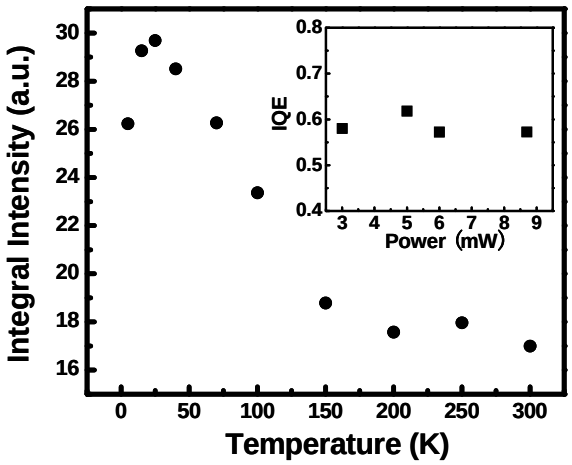

Figure 6. Variation of the integrated PL intensity from the InN core as a function of the measurement temperature under an excitation power of 8.7 mW. The internal quantum efficiency (IQE) as a function of excitation laser power is shown in the inset.

2.5. Self-Organized InAs/InGaAsP Quantum Dot Tube Lasers

An alternative approach to achieve high performance 1.55 μm nanoscale lasers on Si is to utilize rolled-up tube structures. Such nanoscale devices can be realized by utilizing InN/InGaN or InAs/InGaAsP nanomembranes. During this course of this short-term project, we have investigated the fabrication and performance characteristics of self-organized InAs/InGaAsP quantum dot tube lasers.

Coherently strained InGaAsP bilayers, consisting of 38 nm $In_{0.81}Ga_{0.19}As_{0.41}P_{0.59}$ and 15 nm $In_{0.68}Ga_{0.32}As_{0.41}P_{0.59}$ are first grown on an InP substrate. Two layers of self-organized InAs quantum dots are incorporated as the gain medium. To realize free-standing tube cavities, a U-shaped mesa, first defined by etching up to the $In_{0.81}Ga_{0.19}As_{0.41}P_{0.59}$ layer using $HCl:HNO_3:H_2O$ (1:2:1) solution. Subsequently, with a selective etching of the underlying InP layer, the strained

mesa can be controllably released from the substrate. Scanning electron microscopy images of the surface corrugations as well as a side view of the tube device are shown in Figures 7(b) and (c), respectively. In this study, we have focused on InAs/InGaAsP quantum dot tube devices with diameters of ~5 μm, wall thicknesses between 50 to 100 nm, and varying parabolic-like surface geometries.

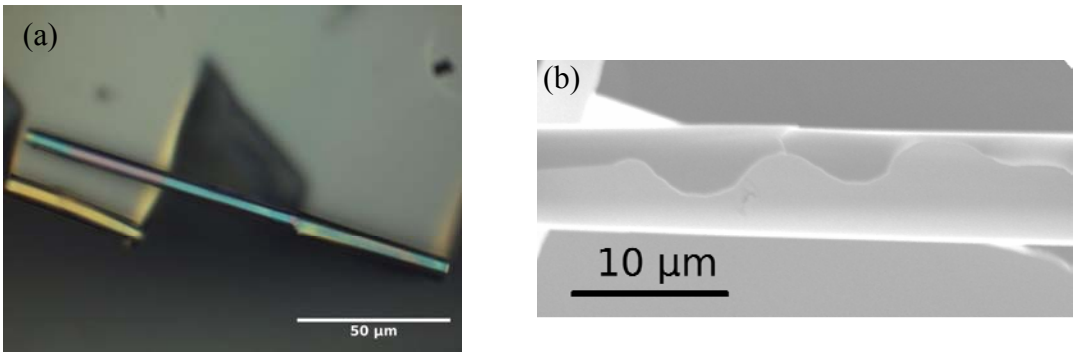

Figure 7: (a) Scanning electron microscopy image showing a detailed view of the surface modifications on a tube structure. (b) Scanning electron microscopy image displaying a side view of a tube device.

We have achieved lasing for a rolled-up tube cavity with a wall thickness of ~100 nm and a tube diameter of nearly ~ 5 μm at 82 K. The emission spectra measured at two different excitation powers (~ 0.18 μW and 5.8 μW) are shown in Figure 8(a). Also shown in the figure, as a reference, is the photoluminescence spectrum measured from as-grown InAs/InGaAsP quantum dot structures. Both tube spectra show clear mode structures, with very little background emission from the quantum dots, indicating a good coupling between the quantum dot photoluminescence emission and the optical modes. The associated azimuthal (m) and axial (p) mode numbers are also identified.

We measured spectra at different pump excitation levels to study the power-dependent behavior. The emission peaks are further analyzed by fitting with Lorentzian functions. Variation of the integrated intensity vs. the pump power for mode (22,1) is shown in Figure 8(b) as red circles. The light-light curve shows a clear kink, from which we estimated a 1.26 μW lasing threshold. Illustrated in the inset of Figure 8 is the measured spectral linewidth that shows a clear reduction (from ~ 2.2 to 1.8 nm) at or near the lasing threshold. This linewidth narrowing, due to the increased temporal coherence, further suggests the achievement of lasing. It is also important to notice that the intrinsic linewidth can be substantially smaller, due to the presence of doublet modes related to the spiral asymmetry of rolled-up semiconductor tubes. We have further calculated the integrated background emission to evaluate its behavior at different pump powers, shown as diamonds in Figure 8. We chose a spectral width of 4 nm, separated from the lasing peak by 8 nm, such that this spectral range is still approximately within the homogeneous broadening limit of the lasing mode. This spectral area is marked by the square box shown in Figure 8(a). It is seen that, at or near the lasing threshold (between 1 and 2 μW), the background emission stays nearly constant which is in direct contrast to the sharp increase of the intensity for the lasing mode (22,1). This observation is consistent with the fact that, for a semiconductor laser, the carrier density above threshold should be clamped at that of the threshold, thereby providing unambiguous evidence for the achievement of lasing. With further increasing power,

the background emission shows a very small increase, with a slope more than 100 times smaller than that of the light-light curve for mode (22,1). This small increase can be explained by the commonly observed hot carrier effect of quantum dot lasers. At large injection conditions, charge carriers are thermally distributed into the many available states and can lead to enhanced background emission.

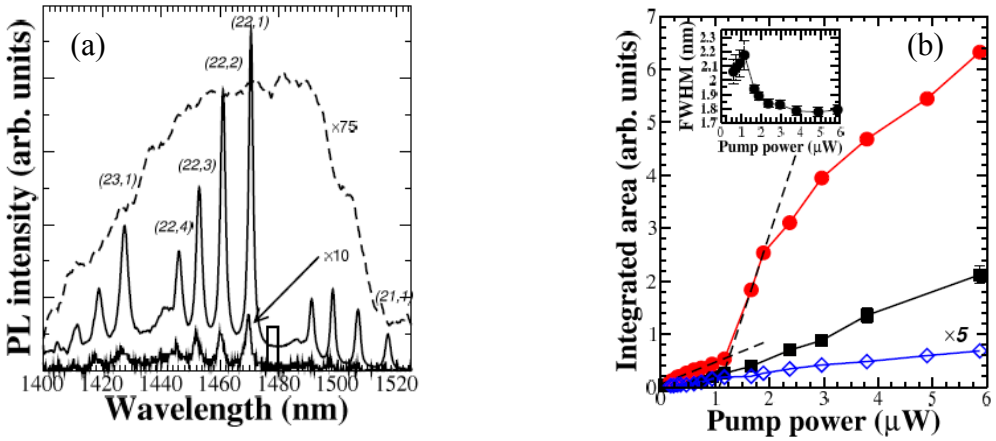

Figure 8: (a) Photoluminescence spectra of a tube device measured at 82 K. The lower (weaker) spectrum corresponds to a small absorbed pump power of ~ 180 nW, while the upper (stronger) one was measured at a high absorbed pump power of ~ 5.6 μW. The low-intensity spectrum has been multiplied by 10 to improve its visibility. The dashed line represents the spectrum (multiplied 75 times, for better visibility) of an as-grown quantum dot heterostructure measured at the same temperature for reference. (b) Light-light curve for mode (22,1) (circles) and (22,4) (squares) shown in (a). Mode (22,1) shows a lasing threshold of 1.26 μW. The dashed lines are a guide to estimate the threshold power. Mode (22,4) shows no threshold behavior. Inset: Linewidth of mode (22,1) as a function of pump power. The background emission extracted from the box in (a) (multiplied by a factor of 5 for better visibility) is indicated by diamonds. Light-light curve for mode (22,4) in Figure 4, showing no threshold behavior.

Also illustrated in Figure 8(b) as black squares, the light-light characteristics of mode (22,4) are examined. The integrated peak area increases linearly with pump power, with no appreciable kinks. From this observation, we can conclude that this particular mode is not lasing. The fact that this mode does not show lasing behavior rules out experimental artifacts during the measurement as the cause of the observed lasing behavior of mode (22,1). It is envisioned that rolled-up semiconductor tube lasers, with multiple emission wavelengths and controlled emission characteristics, can be readily achieved using tube cavities with improved Q-factors by optimizing wall thicknesses and surface geometry.

In summary, we have demonstrated that InN nanowire heterostructures grown directly on Si substrate can exhibit well-controlled structural, electrical and optical properties. The realization of intrinsic InN, tunable surface charge properties, and InN/InGaN core/shell structures has addressed some of the major roadblocks for achieving electrically injected 1.55 μm nanowire lasers on Si. It may also be noted that the growth temperature of InN is generally in the range of ~ 400 – 500 °C, which is compatible with or below the CMOS thermal budget. We have also demonstrated self-organized InAs quantum dot tube lasers that can operate in the wavelength range (S band) suitable for optical communications.

3. List of Publications

1. S. Zhao, S. Fathololoumi, K. H. Bevan, D. Liu, Md. G. Kibria, Q. Li, G. Wang, H. Guo, and Z. Mi, "Tuning surface charge properties of epitaxial InN surfaces," *Nano Lett.,* vol. 12, pp. 2877-2882, 2012.
2. P. Bianucci, S. Mukherjee, M. H. T. Dastjerdi, P. J. Poole, and Z. Mi, "Self-organized InAs/InGaAsP quantum dot tube lasers," *Appl. Phys. Lett.,* vol. 101, 033104, 2012.
3. K. Cui, S. Fathololoumi, Md. Golam Kibria, G. A. Botton, and Z. Mi, "Molecular beam epitaxial growth and characterization of InN/$In_xGa_{1-x}N$ core/shell nanowire heterostructures on Si(111) substrates," *Nanotechnol.,* vol. 23, 085205, 2012.
4. P. Bianucci, M. H. Tavakoli-Dastjerdi, S. Mukherjee, M. Djavid, P. J. Poole, Z. Mi "An optically pumped InGaAsP/InP quantum dot rolled-up microtube laser", *American Physical Society March Meeting*, Boston, MA, Feb. 27 - March 2, 2012.
5. Invited: Z. Mi, P. Bianucci, M. H. T. Dastjerdi, S. Mukherjee, M. Djavid, and P. Poole, "Rolled-up 1.55 μm Semiconductor Quantum Dot Tube Lasers", *221st Electrochemical Society Meeting*, Seattle, WA, USA, May 6-11, 2012.
6. S. Zhao, S. Fathololoumi, K. H. Bevan, D. Liu, Md. G. Kibria, Q. Li, G. Wang, H. Guo, and Z. Mi, "Tuning the surface charge properties of InN nanowires," *Electronic Materials Conference*, Pennsylvania State University, June 20-22, 2012.
7. S. Zhao, S. Fathololoumi, K. Cui, Q. Li, G. Wang, and Z. Mi, "Molecular beam epitaxial growth and characterization of nearly intrinsic and Si-doped InN nanowires," *Photonics West Conference*, San Francisco, CA, Jan. 21-26, 2012.

4. Report of Inventions

None.

5. List of Scientific Personnel Supported, Degrees, Awards and Honors

Zetian Mi received the Christophe Pierre Award for Research Excellence in the Faculty of Engineering at McGill University in 2012.

6. Technology Transition

None.